

Control of a Space Rigidizable-Inflatable Boom Using Embedded Piezoelectric Composite Actuators

Pablo A. Tarazaga, Daniel J. Inman
Center for Intelligent Material Systems and Structures, Virginia Polytechnic Institute and State University
310 Durham Hall, MC 0261, Blacksburg, VA 24061

and

W. Keats Wilkie
Jet Propulsion Laboratory, California Institute of Technology
4800 Oak Grove Drive, MS 299-101, Pasadena, CA 91109-8099

An experimental investigation of vibration testing and active control of a space rigidizable inflatable composite boom containing embedded piezoelectric composite actuators was conducted. Inflatable deployable space structures offer reduced mass, higher packaging efficiency, lower life cycle cost, simpler design with fewer parts, and higher deployment reliability for many large deployable spacecraft structures applications. Enhancing deployed precision and repeatability for these structures is an ongoing research area; in particular, for rigidizable inflatable material systems. In this study we demonstrate in situ vibration testing and active damping using piezoelectric Macro-Fiber Composite actuators embedded within a typical space-rigidizable deployable composite boom. The embedded Macro-Fiber Composite are shown to be capable of surviving integration, packaging, deployment and thermal rigidization in vacuum, and subsequently operating at their full actuation capability. Positive position feedback controllers using accelerometer, laser vibrometer, and strain gage feedback signals are designed and experimentally evaluated. Velocity-proportional and acceleration proportional controllers shown to be capable of attenuating fundamental bending response significantly using only modest control authority (-23dB with 10% of available voltage).

Keywords: PPF, PVF, PAF, piezoelectric actuators, Macro-Fiber Composite, rigidizable structures

1. Introduction

Space inflatable structures are a promising technology that can potentially revolutionize the design of large satellite systems. For many large deployable space structures applications, space inflatable structures have many advantages over mechanically deployed systems, such as lighter weight, higher packaging efficiency, lower life cycle cost, lower parts counts, and higher deployment reliability. Advantages like these have sparked great interest in these inflatable structures and the proliferation of papers in this area as reviewed by Freeland et al. 1998 and lately by Ruggiero et al. 2004. However, space rigidization, modeling, control and deployment of inflatable structures continues to be a major technical challenge (Lou et al. 2000, Lou et al. 2002, Fang et al. 2003).

A common approach to the inflatable space structure starts with a basic component referred to, or known as, inflatable booms. They are the basic building blocks of these structures and are characterized by being long, tubular inflatable beams and struts. The advantages they bring are that in general they are flexible and can be rolled up or folded to achieve high packing efficiency. After the desired orbital location has been reached the stowed booms are inflated and deployed by internal pressurization to attain their intended geometrical shape. At this point there are two main types of inflatable booms. One in which the pressure is maintained to keep the boom in its intended shape or the other that rigidizes and eliminates the need for internal pressure. This research focuses mainly on rigidizable booms (Harrah et al. 2004, Cadogan 2001, Cobb et al. 2004, Freeland et al. 2004). They are subsequently rigidized by one of several methods. In the case of thermoset resin systems, the polymer matrix of the composite structure is cured in situ using integrated electric heaters, or in some instances using incident ultraviolet solar radiation (Allred et al. 2002). Other rigidizable composites use “sub- T_g ” or shape memory polymer thermoplastic resins.

Vibration suppression is a great concern in large space inflatable structures (Park et al. 2002, Park et al. 2001). Once deployed, these inflatable structures are subject to vibrations that can be induced mechanically by satellite repositioning, space debris and thermally induced vibrations due to the change in sunlight from entering and exiting earth's shadow. Controlling these space structures presents a great challenge (Jenkins 2000) but is often necessary to do so in order to ensure optimal performance.

Dynamics testing of very lightweight inflatable structures can be non-trivial and a great deal of effort has gone into developing practical test methodologies for characterizing the properties and deployment characteristics of inflatable structures (Ruggiero et al. 2004). Piezoelectric composite actuators such as the AFC (Bent et al. 1997) and MFC have proven to be useful tool for vibration suppression and dynamic testing of a variety of aerospace structures (Sodano et al. 2004, Wilkie et al 2000). MFC piezocomposites, developed by NASA Langley Research Center consist of a single layer of precision machined piezoelectric fibers in a polymer matrix. Piezoelectric fibers are usually manufactured from a piezoelectric ceramic wafer. Lead zirconate titanate (PZT) compositions are most often employed, although other piezoelectric materials, e.g., PMN-PT single-crystal, may be used. The fibers and matrix are packaged between two polyimide films patterned with an array of interdigitated electrodes. The composite construction of improves the durability and toughness of the encased piezoceramic fibers, which are ordinarily very brittle. The resulting composite package is also more flexible and conformable than, for example, monolithic piezoceramic wafers. This permits them to be integrated within or bonded too curved surfaces relatively easily. This durability and flexibility is ideal for use in vibration applications with inflatable, rigidizable composites, where surfaces are curved and undergo large deformations during inflation and subsequent on-orbit curing and rigidization

This paper defines two controllers, *positive velocity feedback* and *positive acceleration feedback*, following the concept of a *positive position feedback* controller (Goh et al. 1985) and investigates the stability properties of each. Following this several experiment are conducted to implement all three controllers.

2. PPF, PVF and PAF

Positive Position Feedback (Goh et al. 1985) is a widely used form of control, for its ease of use and effectiveness. Among some advantages, *positive position feedback* (PPF) does not need a model of the structure or plant trying to be controlled. The controller can be designed around the experimental transfer function of the structure, making it popular among experimentalist and structural control engineers. These controllers are designed to roll off at higher frequencies and avoid exiting residual modes and spillover.

Consider a single degree of freedom system (alternatively a single decoupled mode of the system) defined as

$$\ddot{x} + 2\zeta\omega_n\dot{x} + \omega_n^2x = bu. \quad (1)$$

where ζ and ω_n are the damping ratio and natural frequency of the structure, and b is the input coefficient that determines the level of force applied to the mode of interest. The PPF controller is implemented using an auxiliary dynamical system defines as

$$\begin{aligned} \ddot{\eta} + 2\zeta_f\omega_f\dot{\eta} + \omega_f^2\eta &= g\omega_f^2x \\ u &= \frac{g}{b}\omega_f^2\eta \end{aligned} \quad (2)$$

where ζ_f and ω_f are the damping ratio and natural frequency of the controller and g is a constant. These parameters are left to the designer to manipulate and obtain the best controller possible. Combining equations (1) and (2) and placing them in their second order form assuming no external forces gives us

$$\begin{bmatrix} \dot{x} \\ \dot{\eta} \end{bmatrix} + \begin{bmatrix} 2\zeta\omega_n & 0 \\ 0 & 2\zeta_f\omega_f \end{bmatrix} \begin{bmatrix} \dot{x} \\ \dot{\eta} \end{bmatrix} + \begin{bmatrix} \omega_n^2 & -g\omega_f^2 \\ -g\omega_f^2 & \omega_f^2 \end{bmatrix} \begin{bmatrix} x \\ \eta \end{bmatrix} = \begin{bmatrix} 0 \\ 0 \end{bmatrix}. \quad (3)$$

Previous work was done by Caughey and Goh (1985) and Caughey (1995) with a Routh Hurwitz approach for the stability conditions of a PPF controller. Fanson and Caughey (1990) looked at the stability condition for the PPF from a Liapunov approach, which is restated here for the single degree of freedom controller.

To determine the stability of this system one must step back and define such conditions. For a conservative system defined by

$$M\ddot{\mathbf{q}} + K\mathbf{q} = 0, \quad (4)$$

where M and K are symmetric, the system is stable if M and K are positive definite. This is simply because the eigenvalues of K are positive and hence the eigenvalues of the system are purely imaginary. Thus, the system is stable since the response of such system is always bounded by a constant.

One can also define a Liapunov function for the system in (4) as

$$V(\mathbf{q}) = \frac{1}{2} [\dot{\mathbf{q}}^T M \dot{\mathbf{q}} + \mathbf{q}^T K \mathbf{q}]. \quad (5)$$

Equation (5) is readily identified as the energy in the system. Stability can now be defined by the following conditions:

$$V(\mathbf{q}) > 0 \text{ for all values of } \mathbf{q}(t) \neq 0$$

$$\dot{V}(\mathbf{q}) \leq 0 \text{ for all values of } \mathbf{q}(t) \neq 0$$

If $\dot{V}(\mathbf{q})$ is strictly less the zero the system is asymptotically stable. One can see now that if M and K are positive definite $V(\mathbf{q}) > 0$, and thus the first condition is met. For the second condition the time derivative of (5) is taken resulting in

$$\frac{d}{dt} V(\mathbf{q}) = \dot{\mathbf{q}}^T M \ddot{\mathbf{q}} + \dot{\mathbf{q}}^T K \mathbf{q}. \quad (6)$$

Multiplying equation (4) on the left by $\dot{\mathbf{q}}^T$ gives us

$$\dot{\mathbf{q}}^T M \ddot{\mathbf{q}} + \dot{\mathbf{q}}^T K \mathbf{q} = 0. \quad (7)$$

Hence the second condition for the Liapunov function is $\dot{V}(\mathbf{q}) = 0$, and thus the equilibrium of equation (4) is stable.

Adding damping to the system in (4) leads to

$$M\ddot{\mathbf{q}} + C\dot{\mathbf{q}} + K\mathbf{q} = 0. \quad (8)$$

$V(\mathbf{q})$ as defined by (5) is still a Liapunov function of (8). In this case the solution $\mathbf{q}(t)$ must satisfy

$$\dot{\mathbf{q}}^T M \ddot{\mathbf{q}} + \dot{\mathbf{q}}^T K \mathbf{q} = -(\dot{\mathbf{q}}^T C \dot{\mathbf{q}}) \quad (9)$$

which comes from premultiplying (8) by $\dot{\mathbf{q}}^T$. From this it can be seen that the time derivative of the Liapunov function is

$$\frac{d}{dt} V(\mathbf{q}) = -(\dot{\mathbf{q}}^T C \dot{\mathbf{q}}). \quad (10)$$

Observing (10) shows that if C is positive definite $\dot{V}(\mathbf{q}) < 0$ and the system in (8) is asymptotically stable. If C is positive semidefinite the above argument is still valid and the system is stable. However, it is not clear if the system is also asymptotically stable. Moran (1970) showed that if none of the eigenvectors of K lie in the null space of C then the system in (8) is asymptotically stable.

Referring back to the system specified in (3) it can be said that this is a stable (asymptotically stable) closed loop system if the symmetric "stiffness" matrix is positive definite for appropriate choices of g and ω_f . That is if the determinant of displacement coefficient matrix is positive which happens if

$$g^2 \omega_f^2 < \omega_n^2.$$

In the case of the PPF the stability conditions depend only on the natural frequency of the system and not on the damping or mode shapes. This is good as natural frequency is the most accurate measurement of these three.

Looking at the transfer function of the controller, in equation (11), one can see that it rolls off at high frequencies avoiding spillover into higher modes, having the characteristics of a low pass filter. The controller transfer function is

$$\frac{\eta(s)}{X(s)} = \frac{g \omega_f}{s^2 + 2\zeta_f \omega_f s + \omega_f^2}. \quad (11)$$

Thus the approach is well suited to control modes that are well separated as the controller is insensitive to higher un-modeled dynamics.

In application the feedback signal can not always be chosen and it is readily determined by what is available or what is more feasible as sensors. Thus, much in the same way one can define a Positive Velocity Feedback (PVF) controller. In this case the controller is defined as

$$\begin{aligned} \ddot{\eta} + 2\zeta_f \omega_f \dot{\eta} + \omega_f^2 \eta &= g \omega_f \dot{x} \\ u &= \frac{g}{b} \omega_f \dot{\eta} \end{aligned} \quad (12)$$

Combining equations (1) and (12) and placing them in their second order form assuming no external forces gives us

$$\begin{bmatrix} \ddot{x} \\ \ddot{\eta} \end{bmatrix} + \begin{bmatrix} 2\zeta \omega_n & -g\omega_f \\ -g\omega_f & 2\zeta_f \omega_f \end{bmatrix} \begin{bmatrix} \dot{x} \\ \dot{\eta} \end{bmatrix} + \begin{bmatrix} \omega_n^2 & 0 \\ 0 & \omega_f^2 \end{bmatrix} \begin{bmatrix} x \\ \eta \end{bmatrix} = \begin{bmatrix} 0 \\ 0 \end{bmatrix} \quad (13)$$

It is seen that in this case the stability conditions have moved to the damping matrix. Because of the velocity feedback no longer is the stiffness matrix affected by the controller. In this case the stability conditions are more relaxed, since the condition for stability requires that the damping matrix be positive semidefinite (Inman 1989). Looking at the determinate of the velocity coefficient matrix the following condition arises for stability

$$\zeta \omega_n \geq \frac{g^2 \omega_f}{4\zeta_f} \quad (14)$$

In the case that it is strictly greater than (14) it guarantees asymptotical stability. As stated before Moran (1970) showed that if the eigenvectors of K do not lie in the null space of C the system is asymptotically stable even if C is semidefinite. In the case of equation (13) this is always the case as long as the term $-g\omega_f$ in the “damping” matrix is not equal to zero. The term $-g\omega_f$ could never be zero since it would signify no controller. Thus as long as the condition in (14) is satisfied the system will be asymptotically stable.

The PVF controller also has the roll off characteristic as that of the PPF. Its roll off

though is not as fast as that of the PPF and this can be seen by observing the transfer function for PVF:

$$\frac{\eta(s)}{X(s)} = \frac{g\omega_f^2 s}{s^2 + 2\zeta_f \omega_f s + \omega_f^2} \quad (15)$$

The slower roll off is caused by the s term in the numerator of the transfer function consequential of the velocity feedback.

Again in the similar manner as for the PVF we can design a Positive Acceleration Feedback (PAV) controller as follows,

$$\begin{aligned} \ddot{\eta} + 2\zeta_f \omega_f \dot{\eta} + \omega_f^2 \eta &= g \ddot{x} \\ u &= \frac{g}{b} \ddot{\eta} \end{aligned} \quad (16)$$

Combining equations (1) and (16) and placing them in their second order form assuming no external forces gives us

$$\begin{bmatrix} 1 & -g \\ -g & 1 \end{bmatrix} \begin{bmatrix} \ddot{x} \\ \ddot{\eta} \end{bmatrix} + \begin{bmatrix} 2\zeta \omega_n & 0 \\ 0 & 2\zeta_f \omega_f \end{bmatrix} \begin{bmatrix} \dot{x} \\ \dot{\eta} \end{bmatrix} + \begin{bmatrix} \omega_n^2 & 0 \\ 0 & \omega_f^2 \end{bmatrix} \begin{bmatrix} x \\ \eta \end{bmatrix} = \begin{bmatrix} 0 \\ 0 \end{bmatrix} \quad (17)$$

In this case it is required that the mass matrix be positive definite for stability (asymptotical stability). That leaves the condition that the gain g must be chosen with the following condition for stability

$$g^2 < 1 \quad (18)$$

Unlike the other two controllers this one those not roll off. This can be seen by looking at the transfer function of the controller

$$\frac{\eta(s)}{X(s)} = \frac{gs^2}{s^2 + 2\zeta_f \omega_f s + \omega_f^2} \quad (19)$$

This effect needs to be taken into consideration when using this type of controller since it can disturb the higher modes. Figure 1 shows the frequency response of a 2nd order plant model (solid line) and the controlled closed loop plant using the three methods described above. As we can see the PAF does not roll off. With the design of such controllers we have covered a wide range of sensors that could possibly be used

for feedback in the control of large inflatable satellite structures.

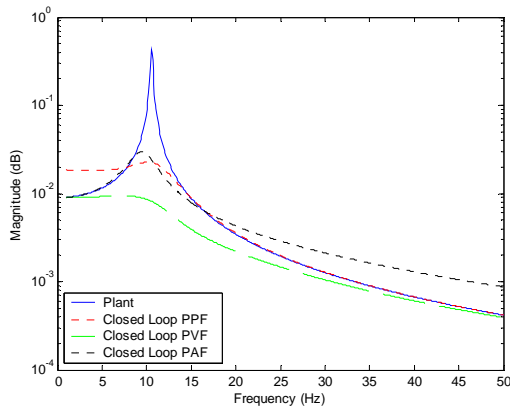


Figure 1. Transfer function of a 2nd order plant and the respective close loop transfer functions using the different controllers.

3. Test Structure

The primary test structure is an inflatable rigidizable boom manufactured by L'GARDE, Inc. The boom consists of three graphite fiber unidirectional plies [0/90/0] in a proprietary thermoset epoxy resin system. Four MFC actuator devices constructed by NASA Langley Research Center are embedded within the composite structure of the boom in a belt configuration near the base. 0.5 mil Kapton internal and external membranes serve as an inflation bladder and inflation shape restraint. The boom is designed to be packaged in a Z-folded arrangement. Once deployed, the epoxy resin is thermally cured to rigidize and consolidate the composite structure including the internal actuators. Deployed dimensions of the boom are 91.122 5 cm (35.875 inches) in length, 10.16 cm (4 inches) inner diameter. Total effective wall thickness is 0.508 mm (0.020 inches). The embedded MFC actuator devices were approximately 86 mm (3.375 inches) long by 57 mm (2.25 inches) wide with PZT-5A piezoceramic fibers oriented along the length of the boom. Machined fiber cross-section dimensions were approximately 0.356 mm by 0.176 mm (0.014 by 0.007 inches) with a separation gap of 0.075 mm (0.003 inches). Total MFC package thickness, including 0.5 mil outer Kapton layers, Pyralux sheet adhesive and 0,5 ounce copper electrodes was 0.264 mm (0.0104 inches). Actuator interdigitated

electrode spacing was 1.07 mm (0.042 inches) center-to-center with a nominal electrode finger width of 0.127 mm (0.005 inches). MFC actuators and flat copper/Kapton wiring leads were positioned within cutouts in the center ply of the composite layup during assembly. Figure 2 shows a typical MFC actuator used for this experiment, and the integrated actuator-boom test article in its packaged state prior to inflation and rigidization.

The packaged boom test article was inflated and thermally cured in a vacuum chamber to demonstrate deployment viability. The boom was later equipped with a PVC pipe 91.44 cm (36 inches) in length, inner diameter 10.16 cm (4 inches) and 6.35 mm (0.25 inches) thick. This was done to approximate the bending dynamics of a 3 meter full-sized inflatable rigidizable boom. Figure 3 shows the inflated and cured test article before and after installation of the PVC extension.

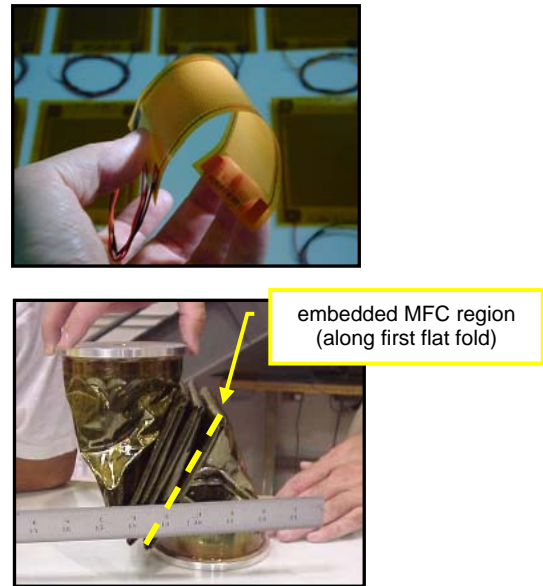


Figure 2. MFC actuator; Z folded, uncured packaged boom with integrated MFC's (Photo credits: (Top) NASA Langley Research Center; (Bottom) L'GARDE, Inc.)

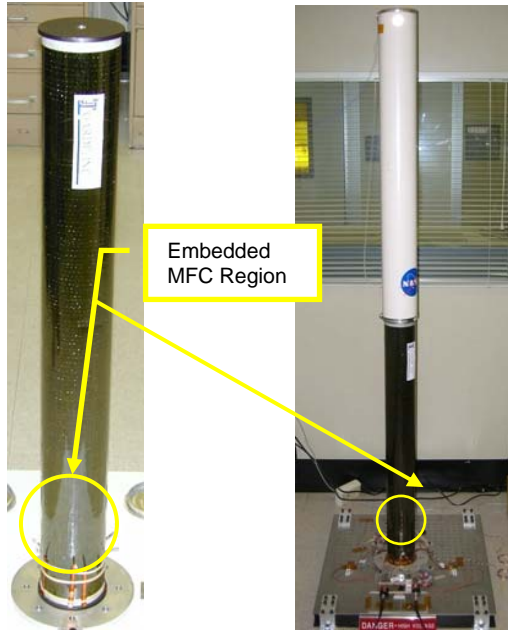


Figure 3. Inflated and rigidized composite test article: (left) after curing;; (right) with PVC extension tube and mounted at the base for vibration testing.

4. Experimental Configuration

The general arrangement of the experimental apparatus is shown in Figure 4. As discussed earlier, the PPF controllers are designed around experimentally determined transfer functions. The primary vibration modes of interest in these experiments were the first and second bending modes of the cantilevered boom. The controller, excitation, and sensor systems are described below.

4.1 Excitation/Disturbance

The excitation administered to the system was performed with one MFC that stretched in the longitudinal direction. Since this is occurring on one side of the boom it produces a bending excitation to the system. Figure 4 designates it as the Excitation/Disturbance MFC.

4.2 Control

The control excitation was administered by the MFC opposite in location to the MFC used for the excitation. In the same manner as the excitation MFC it produces a strain in the longitudinal direction of the boom to counter act

that of the Excitation MFC. Figure 4 designates it as the Control MFC.

4.3 Sensors

Three types of sensing methods; velocity sensing, acceleration sensing, and displacement/strain sensing, were used. The velocity sensing method employed a laser vibrometer (Ometron Model VH300+) to measure the instantaneous velocity of a point near the top of the tube. The laser vibrometer generates an analog voltage signal directly proportional to the normal velocity of the aiming point of the laser. Acceleration sensing was accomplished via a small single-axis accelerometer (PCB 352A21) placed at the top of the tube opposite of the excitation MFC. Displacement sensing was performed using longitudinally oriented foil strain gages (Vishay Measurements Group CEA-06-250WQ-350) bonded to the outside of the tube directly over the centroid of each MFC actuator.

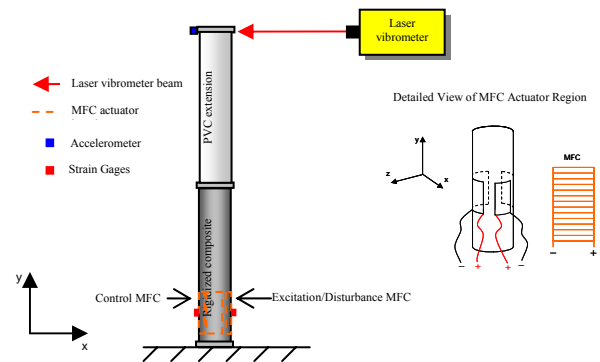


Figure 4. Actuator and sensor schematics of the boom.

5. Results and Analysis

5.1 Frequency Response

Experimental frequency response functions were obtained between the excitation MFC signal and each of the available sensor types. The main experimental objectives were to identify the fundamental bending vibration mode of the composite boom and to verify that the structural dynamic behavior of the system was reasonably linear. An HP/Agilent 35670A Dynamic Signal Analyzer was used to determine the transfer functions. Figure 5 shows characteristic

experimental transfer functions over 0-100 Hz between the MFC actuator excitation signal and the tip accelerometer signal, tip velocity laser vibrometer measurement, and root strain gage signals respectively. The fundamental cantilevered bending mode was located at 10.5 Hz and the second bending mode was located at 58.5 Hz. The frequency response function obtained using the strain gage signal (c) is not as well defined as the other two. The noise level in this reading could be a factor for the small peaks in this case.

A simple linearity check was also performed to verify that the structural dynamic response of the boom and actuator system were reasonably linear. These were accomplished by examining the experimental frequency response functions between the excitation MFC actuator and the laser vibrometer tip velocity measurement for several different excitation amplitudes. Resulting frequency response functions for excitation voltage amplitudes between 150 V and 250 V are shown in Figure 6. The transfer functions are seen to be essentially identical, implying good linearity in the system structural dynamic response.

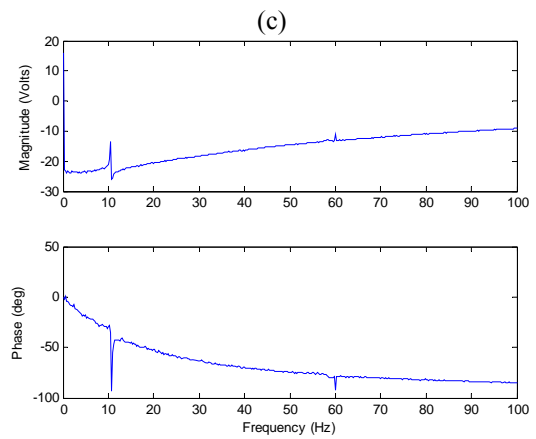
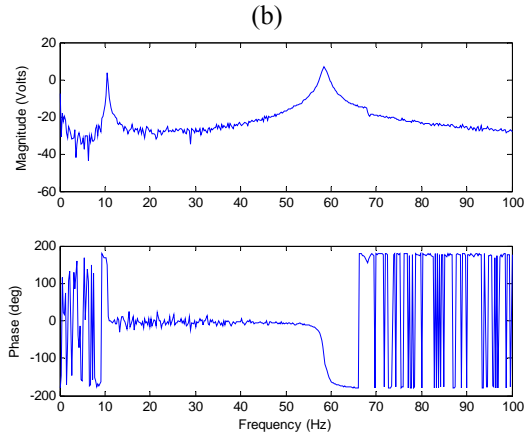
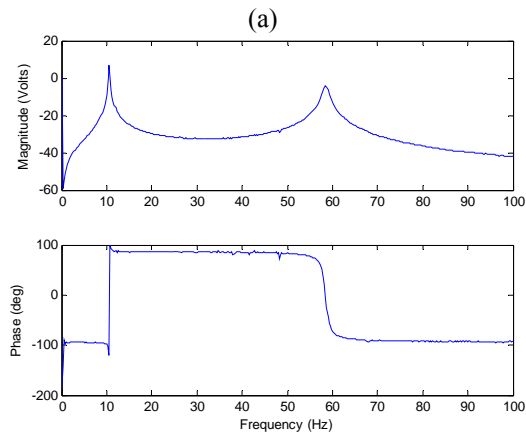


Figure 5. Frequency response functions between the excitation MFC actuator and (a) laser vibrometer sensor, (b) accelerometer sensor, and (c) strain gage sensor located above the excitation actuator.

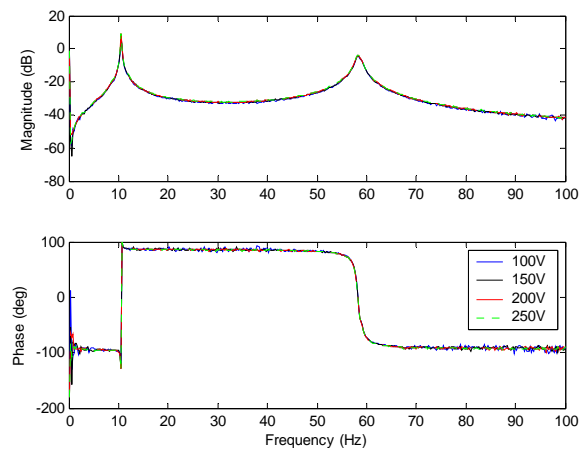


Figure 6. Excitation MFC input to laser vibrometer output transfer function: response amplitude linearity check.

5.2 Controller design

The primary control design objective was to attenuate the vibratory response of the first boom bending mode. Extension of this technique to multiple modes is simple and follows the same idea with cascading filters.

Feedback controllers were implemented using a dSPACE real-time digital control system. A MATLAB/Simulink-based front end was used for control design and programming. Controller gains using velocity proportional, acceleration proportional, and displacement (strain) proportional feedback signals were modified in real-time in order to optimize closed-loop performance. For each control signal case, the controller parameters were modified to obtain the best attenuation possible of the first mode. The controller parameters were control frequency (ω_f), control damping (ζ_f), and control gain (g). The optimal choices for these parameters were determined by observing the experimental frequency response between the excitation MFC input signal and output sensor while manually varying the controller parameters.

The first case examined utilized the laser vibrometer to provide a velocity-proportional feedback signal. Figure 7 (a) illustrates the variations in the experimental transfer function as the controller parameters are adjusted. Figure 7(b) shows the resulting optimal controller response compared with the uncontrolled response. A very large, 23 dB attenuation in the first bending mode response is demonstrated using the optimized controller parameters.

After determining the optimal controller in the frequency domain, its effectiveness was evaluated in the time domain. A sinusoidal disturbance at 10.5 Hz was applied to the structure with the excitation MFC. The laser vibrometer was used to read the response of the structure at the top of the boom. Figure 8 shows the time response before and after the controller was engaged. A 93% reduction in the response amplitude at the tip of the boom is shown.

The same procedure was used to tune the *positive acceleration feedback* (PAF) controller using the tip accelerometer as the feedback sensor. Figure 9 shows the results for this case. Approximately 25 dB reduction in the

acceleration frequency response at the 10.5 Hz first mode resonance was attained, with a corresponding 91% attenuation in the time history signal.

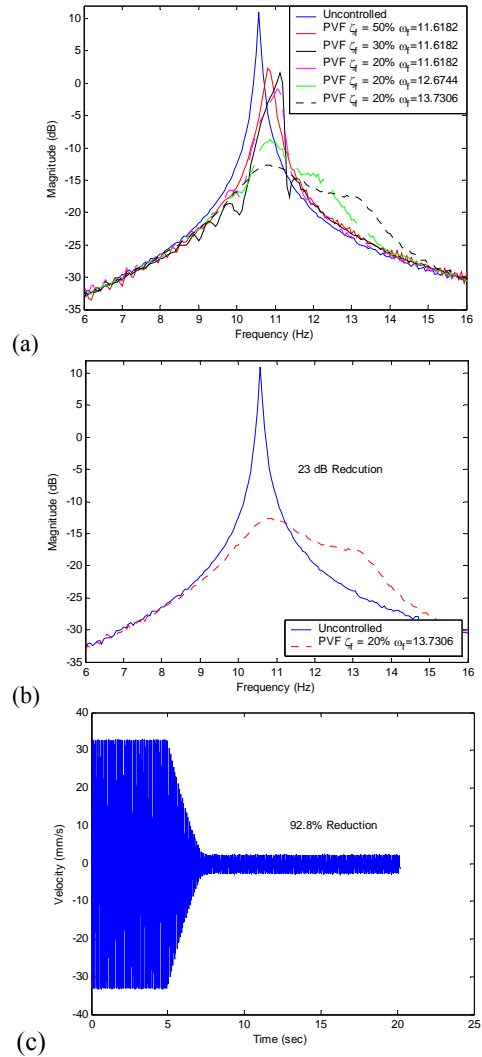


Figure 7. (a) Tuning of the *positive velocity feedback* (PVF) controller; (b) response obtained with the optimal PVF controller parameters; (c) velocity time history at the tip of the boom before and after the optimal PVF controller is engaged (10.5 Hz excitation input).

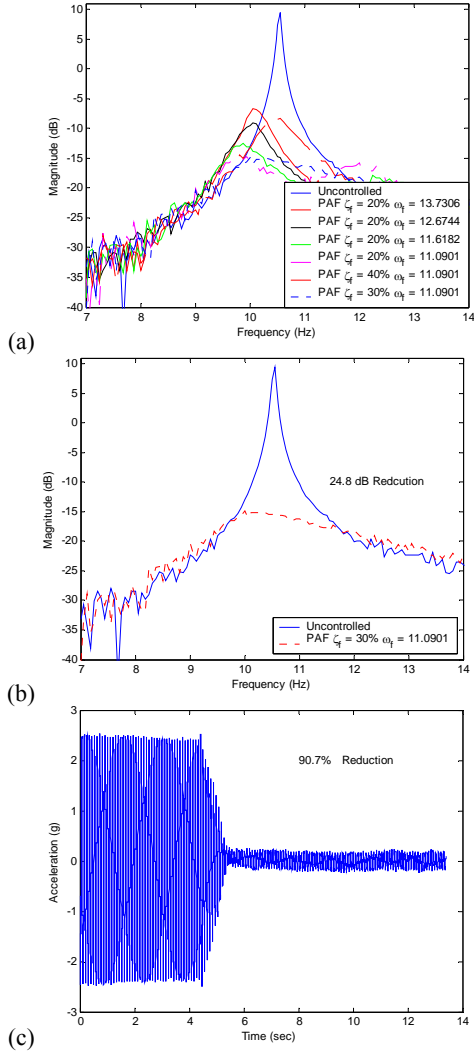


Figure 8. (a) Tuning of the *positive acceleration feedback* (PAF) controller; (b) optimal result in frequency domain; (c) tip accelerometer time history before and after controller is engaged (10.5 Hz excitation input).

The control optimization procedure was repeated using the strain gage sensors. Figure 9 (a) shows the tuning procedure using the signal from the strain gage located on the same side of the boom as the actuation MFC. Figure 9 (b) shows the optimal controller for that case. Figure 9 (c) shows the frequency response for the optimal controller using the signal from the strain gage located on the opposite side of the excitation actuator. In both cases the controller was able to significantly reduce the observed vibration response at the target frequency, although using strain gages placed at a location with a larger modal strain response would yield better results. As the signal-to-noise quality of the strain

responses was typically poor, the optimal strain-feedback PPF controller was also evaluated by examining the resulting effect on the laser vibrometer signal measured at the boom tip. The results are shown in Figure 10 using the signal from the opposite-side strain gage for the controller feedback. Some attenuation is shown in the net vibrational response at the boom tip, although this controller is not as effective as either the PVF or PAF controller implementations.

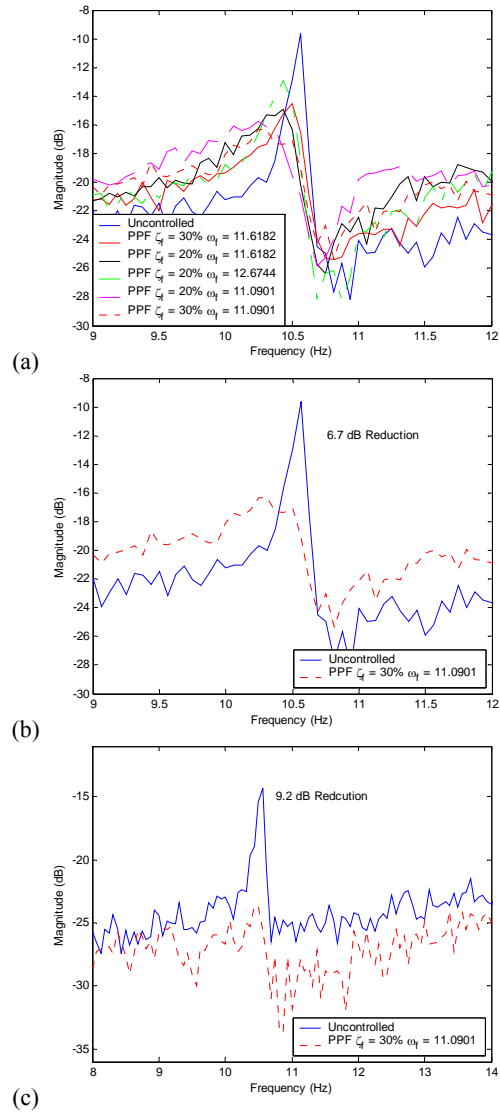


Figure 9. (a) Tuning of the *positive position feedback* (PPF) controller using the strain gage located on the same side as the excitation MFC; (b) optimal result for PPF using the same-side strain gage signal; (c) optimal controller result using the strain gage on the opposite side of the excitation MFC.

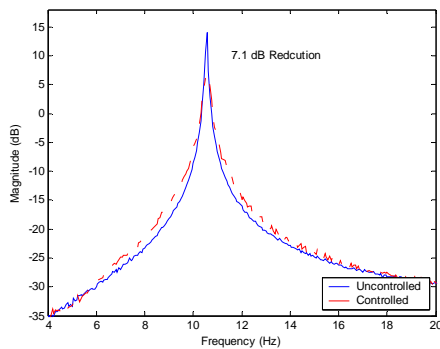


Figure 10. Frequency response function between the actuation MFC and the laser vibrometer while using strain gage as feedback for the controlled case.

6. Conclusions

The use of embedded Macro-Fiber Composite (MFC) piezocomposites for vibration suppression on a space inflatable-rigidizable boom was successfully demonstrated using “positive position feedback” (PPF) closed-loop control. MFC actuators were shown to be capable of surviving the composite integration, folding and packaging, vacuum deployment and thermal rigidization processes used with a typical space inflatable-rigidizable structures concept and subsequently operating at their full capacity. PPF architecture controllers employing velocity, acceleration, and displacement (strain) feedback were successfully implemented. Velocity and acceleration-based feedback PPF controllers were able to attenuate the first mode almost to noise level using only modest control voltages. Comparable performance with half the voltage amplitude can be expected for all controllers using more current MFC electrode architectures. Results for positive acceleration feedback controllers were particularly encouraging as acceleration signals are much easier to obtain on actual flight structures than velocity-proportional signals. For the strain-based *positive position* feedback cases, some reduction in the vibration response was achieved, although alternative locations for the strain gage sensors should yield more effective controllers.

Acknowledgments

The authors wish to express their thanks to the following individuals who contributed greatly to this effort: Billy Derbes (L’GARDE, Inc.), Richard Helms and Robert Freeland (JPL), Jason

Hinkle and Martin Mikulas (University of Colorado at Boulder), and James High and Richard Pappa (NASA Langley Research Center). This work was sponsored in part by the National Aeronautics and Space Administration GSRP Fellowship program and the Virginia Tech G.R. Goodson Professorship.

Reference

1. Allred, R., Hoyt, A., McElroy, P., Scarborough, S., and Cadogan, D., 2002, “UV -Rigidizeable Carbon-Reinforced Isogrid Inflatable Booms,” in *43rd 42nd AIAA/ASME/ASCE/AHS/ASC Structures, Structural Dynamics, and Materials Conference*, 22-25 April, Denver CO.
2. Bent, Aaron, A., Hagood, Nesbitt, W., 1997, “Piezoelectric Fiber Composites with Interdigitated Electrodes.” *Journal of Intelligent Material Systems & Structures*. v 8 n 11 Nov. pp. 903-919.
3. Cadogan, D., 2001, “Rigidization Materials for use in Gossamer Space Inflatable Structures,” in *42nd AIAA/ASME/ASCE/AHS/ASC Structures, Structural Dynamics, and Materials Conference*, April 16-19, Seattle, WA, pp. 2001-1417.
4. Caughey, T., K., 1995, “Dynamic Response of Structures Constructed from Smart Materials,” in *Smart Materials and Structures*, March, 4 No 1A A101-A106.
5. Cobb, R., Lindemuth, S., Slater, J., 2004, “Development and Test of a Rigidizable Inflatable Structure Experiment,” in *Structural Dynamics & Materials Conference*, Palm Springs, California, April 19-22, 2004.
6. Fang, H., Lou, M., and Hah, J., 2003, “Deployment Study of a Self-Rigidizable Inflatable Boom,” *44th /ASME/ASCE/AHS/ASC Structures, Structural Dynamics, and Materials Conference*, 7-10 April, Norfolk, VA.
7. Fanson, J., L., and Caughey, T., K., 1990, “Positive Position Feedback Control for Large Space Structures,” in *AIAA Journal* April, Vol. 28 No. 4.
8. Freeland, R., Helms, R., Willis, P., Mikulas, M., Stuckey, W., Steckel, G., Watson, J., 2004, “Inflatable Space Structures Technology Development for Large Radar Antennas,” *55th International Astronautical Congress*, Vancouver, Canada.
9. Freeland, R., Bilyeu, G., Veal, G., and Mikulas, M., 1998, “Inflatable Deployable Space Structures Technology Summary,” *IAF-98-1.5.01 49th Congress of the*

- International Astronautical Federation, Melbourne, Australia, Sept. 28-Oct. 2.
10. Goh, C. J., Caughey, T. K., 1985, "On the stability Problem Caused by Finite Actuator Dynamics in the Control of Large Space Structures," in *International Journal of Control*, vol. 41, No. 3, pp. 787-802.
 11. Harrah, L. A., Hoyt Haight, A. E., Sprouse, M. R., Allred, R. E., McElroy, P. M., Scarborough, S., Dixit, A., 2004, "Resin and Manufacturing Development for Light Curing Inflatable Composite Booms. 45th /ASME/ASCE/AHS/ASC Structures, Structural Dynamics, and Materials Conference, 19-22 April, Palm Springs, Ca.
 12. Inman, D. J., 1989, "Vibration: With Control, Measurement, and Stability". Prentice Hall 1989.
 13. Jenkins, C. H., Kalanovic, V. D., 2000, "Issues in Control of Space Membrane/Inflatable Structures," in *IEEE Aerospace Conference Proceedings. v 7 2000. p 411-414 (IEEE cat n 00TH8484)*.
 14. Lou, M. Fang, H. Hsia, L -M., 2000, "A Combined Analytical and Experimental Study on Space Inflatable Booms," in *IEEE Aerospace Conference Proceedings. v 2 2000. p 503-512 (IEEE cat n 00TH8484)*.
 15. Lou, M. Fang, H. Hsia, L -M., 2002, "Self-Rigidizable Space Inflatable Boom," *Journal of Space Craft and Rockets. Vol. 39, No.5, September-October.*
 16. Moran, T. J., 1970, "A simple Alternative to the Ruoth-Hurwitz Criterion for Symmetric Systems," in *ASME Journal of Applied Mechanics, 37:1168-1170.*
 17. Park, G., Eric Ruggiero, and Daniel J. Inman., 2002, "Dynamic Testing of an Inflatable Structure Using Smart Materials," in *Smart Materials and Structures, Vol. 11, No. 1, pp. 147-166.*
 18. Park, G., Kim, M., Mandin, M., and Inman, D., J., 2001, "Vibration control of inflatable space structures using smart materials," in *Proceedings 18th ASME Biennial Conf. on Mechanical Vibration and Noise, Pittsburgh, PA, Sep. 9-12, (DETC2001/VIB-21540).*
 19. Ruggiero, Eric J. and Inman, D. J., 2004, "Gossamer Spacecraft: Recent Trends in Design, Analysis, Experimentation, and Control," in *Journal of Spacecraft and Rockets*, submitted February 2004.
 20. Ruggiero, E. J., Tarazaga, P. A., and Inman, D.J., 2004. "Modal Analysis of an Ultra-Flexible, Self Rigidizing Toroidal Satellite Component". *Proceedings of 2004 ASME International Mechanical Engineering Congress and Exposition, November 13-19, Anaheim, CA.*
 21. Sodano, Henry A. Park, Gyuhae. Inman, Daniel J., 2004, "An Investigation Into the Performance of Macro-Fiber Composites for Sensing and Structural Vibration Applications," in *Mechanical Systems & Signal Processing, May, v 18 n 3. p 683-697.*
 22. Wilkie, W Keats. Bryant, Robert G. High, James W. Fox, Robert L. Hellbaum, Richard F. Jalink, Antony Jr. Little, Bruce D. Mirick, Paul H., 2000, "Low-cost Piezocomposite Actuator for Structural Control Applications" *Proceedings of SPIE - The International Society for Optical Engineering, Bellingham, WA, v 3991 p 323-334.*